Journal of Mineralogical and Petrological Sciences, Volume 99, page 118–129, 2004

High-pressure single crystal X-ray diffraction and FT-IR observation of natural chondrodite and synthetic OH-chondrodite

Takahiro KURIBAYASHI*, Hiroyuki KAGI**, Masahiko TANAKA***, Mizuhiko AKIZUKI* and Yasuhiro KUDOH*

*Institute of Mineralogy, Petrology and Economic Geology, Graduate School of Science, Tohoku University, Sendai 980-8578, Japan
**Laboratory for Earthquake Chemistry, Faculty of Science, University of Tokyo, Tokyo 113-0033, Japan
***Institute of Material Structure Science, High Energy Accelerator Research Organization, KEK, Tsukuba 305-0801, Japan

High-pressure single crystal X-ray diffraction studies of a natural chondrodite, $Mg_{4.76}Fe_{0.22}Ti_{0.02}Si_{1.99}O_8(OH_{1.26}F_{0.74})$, and a synthetic OH-chondrodite, $Mg_{4.98}Si_{2.01}H_{2.00}O_{10}$, were performed using a diamond anvil cell (DAC) up to 7.3 and 5.9 GPa, respectively and at room temperature. FT-IR spectra of the natural chondrodite under high-pressure conditions up to 9.9 GPa was also observed using a DAC. The axial linear compressibilities of these samples are calculated as $\beta_a = 1.69(4) \times 10^{-3}$, $\beta_b = 2.98(4) \times 10^{-3}$ and $\beta_c = 2.74(5) \times 10^{-3}$ (GPa^{-1}) for the natural chondrodite and $\beta_a = 2.11(18) \times 10^{-3}$, $\beta_b = 2.83(18) \times 10^{-3}$ and $\beta_c = 3.04(38) \times 10^{-3}$ (GPa^{-1}) for the synthetic OH-chondrodite. The isothermal bulk moduli of these samples were calculated as $K_T = 124.1(4)$ GPa for the natural chondrodite and $K_T = 117(2)$ GPa for the OH-chondrodite, by using the Birch-Murnaghan equation of state assuming $K' = 4$. The bulk moduli of total void space in each sample, assuming $K' = 4$, were calculated to be $K_\square = 116(2)$ GPa for the natural chondrodite and $K_\square = 113(4)$ GPa for the OH-chondrodite. The plots of bulk modulus versus the summation of the filling-factor of polyhedral sites show a good correlation between the humite minerals. This relationship can be explained by the replacement of $4O^{2-} + Si^{4+} \Leftrightarrow 4(F, OH)^- + \square$ generated in the humite homologous series. In the FT-IR spectra of the natural chondrodite, four OH-stretching vibrational peaks were observed at 3688, 3566, 3558 and 3383 cm^{-1} under ambient conditions. The pressure dependences of the frequency of these peaks up to 9.9 GPa are 2.8(3), 3.9(3), 4.0(3) and –2.1(2) ($cm^{-1}GPa^{-1}$), respectively. With increasing pressure up to 9.9 GPa, the 3383 cm^{-1} peak shifts to lower-frequency positions, whereas the other peaks shift to higher-frequency positions. The shortening of the O5⋯O5 distance, which is not the shared edge between M3 octahedra, related to hydrogen bonding with increasing pressure causes the negative pressure-dependence of the 3383 cm^{-1} peak. The positive pressure-dependence of the remaining IR-peaks is due to the compression of the O5-H bond, and not related to hydrogen bonding with increasing pressure.

Introduction

In the Earth's crust and deep interior, volatile elements, especially "Water (OH or H_2O)", may play significant roles in the hydration and dehydration processes in subduction zones, and in the variations of the elastic and plastic properties of rocks and minerals. For example, Yusa and Inoue (1997) reported that in wadsleyite, the bulk modulus of its hydrous phase (K = 155 GPa) is smaller than that of its anhydrous phase (K = 170 GPa, Li et al., 1996). This was also observed in ringwoodite, a polymorph of Mg_2SiO_4, (Inoue et al., 1998; Wang et al., 2003). Water, which is supplied to rocks and minerals in subduction zones, is transported into the Earth's deep interior by the subduction of oceanic plates as "H_2O and/or OH" in hydrous minerals such as serpentine, phologopite, K-richterite, and others.

Chondrodite (n = 2) is one of "the humite group minerals" with the chemical formula, $nMg_2SiO_4 \cdot Mg(OH, F)_2$ (n = 1, 2, 3 and 4). In nature, fluorine-rich phases of humite minerals are generally found in meta-

T. Kuribayashi, t-kuri@mail.tains.tohoku.ac.jp Corresponding author

morphosed and metasomatized limestones and dolomites, and skarns associated with ore deposits. Titano-chondrodite and titano-clinohumite were found in a xenolith derived from the Earth's upper mantle (Aoki et al., 1976). Fluorine free OH-chondrodite and OH-clinohumite were synthesized under conditions corresponding to the upper mantle (ex. 12 GPa, 1158°C) in the system MgO-SiO_2-H_2O (Yamamoto and Akimoto, 1974, 1977; Burnley and Navrotsky, 1996; Wunder, 1998). Thus, chondrodite is a hydrous mineral stable under upper mantle conditions and would be an important mineral as a reservoir and carrier of water in the Earth's interior.

The crystal structure of chondrodite is based on a slightly distorted hexagonal closest packed anion array, the same as that of forsterite. Ribbe et al. (1968) reported that humite minerals consist of forsterite-like blocks, [Mg_2SiO_3(OH,F)] and brucite-like blocks, [MgO(OH,F)]. On the other hand, Fujino and Takeuchi (1978) suggested that the crystal structures of humite minerals could be composed of alternate layers whose compositions could be expressed by $Mg_{2n-1}Si_nO_{4n-2}$ and MgO(OH, F), n = 1, 2, 3 and 4 (n = 2 for chondrodite).

For the isothermal bulk modulus of chondrodite, Williams (1992) estimated (K = 115 GPa) on the assumption that the bulk modulus (K) of chondrodite is additive between forsterite, sellaite and brucite components. Faust and Knittle (1994) reported that the bulk modulus of natural chondrodite [F/(OH + F) = 0.73] was K_T = 136.2 (8.8) GPa with a pressure derivative K' = 3.7(4) calculated from powder X-ray diffraction data up to about 40 GPa. This value is slightly larger than that of forsterite (K_T = 122.6 GPa with K' = 4.3, Kudoh and Takeuchi, 1985; K_T = 125(2) GPa with K' = 4.0(4), Downs et al., 1996). In contrast, Sinogeikin and Bass (1999) reported that the bulk modulus of natural chondrodite with fluorine [F/(OH + F) = 0.32], obtained using the Brillouin scattering method, was K_s = 118.4(1.6) GPa. Ross and Crichton (2001) reported that the bulk moduli of OH-chondrodite [K_T = 115.7(8) GPa, K' = 4.9(2)] and OH-clinohumite [K_T = 119.4(7) GPa, K' = 4.8(2)] were smaller than that of fluorine-containing chondrodite. Thus, these results suggested that, in a polysomatic series such as the minerals of the humite group, the physical properties (ex. bulk modulus) of a "polysome" could be calculated simply by the average of those of the constituent slabs. Ross and Crichton (2001) discussed the relationship between bulk modulus and water contents of humite minerals on the basis of the chemical formula, but further data on specimens of intermediate compositions are needed to clarify the effect of the substitution of OH ⇔ F on bulk compression. Friedrich et al. (2002) refined the crystal structures of natural F-bearing chondrodite [F/(OH + F) = 0.58] at up to 9.63 GPa by the single crystal X-ray diffraction method and of ($OD_{0.90}F_{1.10}$)-chondrodite at up to 5.27 GPa by the neutron powder diffraction method. They discussed the variations of the geometry of the O-D···O/F hydrogen bond with increasing pressure.

Yamamoto (1977) first determined the hydrogen positions of OH-chondrodite from the analysis of X-ray diffraction data and proposed that the hydrogen atoms would be disordered over the two OH sites. This situation was recently confirmed by the neutron diffraction study of Lager et al. (2001). Williams (1992) observed the FT-IR spectra of natural chondrodite [F/(OH + F) = 0.73] under high-pressure conditions up to about 40 GPa. He found that negative and positive shifts of the OH-stretching vibration peaks with increasing pressure. He deduced that the formation and reinforcement of hydrogen bonding would cause the negative peak shift, and the positive shift would be due to H-H repulsion. Lin et al. (1999) reported the Raman spectra of a synthetic OH-chondrodite and a natural chondrodite with [F/(OH + F) = 0.95]. In both samples, they observed only the positive pressure dependences for OH-stretching frequency with increasing pressure. These findings indicate that the fluorine contents in chondrodite would influence not only the behavior of hydrogen bonding but also the compression mechanism of its structure under high-pressure conditions.

In order to clarify the compression mechanism under high-pressure and its influence on the physical properties, we investigated the crystal structure of chondrodite using single crystal X-ray diffraction and FT-IR spectroscopy under high-pressure conditions with a diamond anvil cell. The effects of hydrogen and fluorine on the structural behavior was also observed during the study.

Experimental procedure

Sample

A natural chondrodite sample (Krantz Collection #Q88, Tohoku University), from the Tilley Foster Mine in Brewster New York, U.S.A., was used for X-ray diffraction and FT-IR spectra measurements. OH-chondrodite was synthesized at 6 GPa and 900°C for 11 hours using a Kawai-type high-pressure apparatus (ERI 2000) at the Earthquake Research Institute, University of Tokyo. The starting material for the synthesis of the OH-chondrodite was a stoichiometric mixture of powders of synthetic forsterite (Mg_2SiO_4) and brucite [$Mg(OH)_2$] with a molar ratio of 2:1. Eight tungsten carbide cubes with 8 mm truncations were used to generate pressure in a 14 mm semi-sintered MgO octahedron with a cylindrical graphite furnace. Temperature was measured by a W3%Re97%/

W25%Re75% thermocouple placed in contact with the capsule. No special care was given to get single crystals of OH-chondrodite. The specimens were quenched by turning off the heating power to the furnace and pressure was released gradually for 8 hours.

Chemical analyses were carried out using an EPMA (JEOL, JXA-8800M) operating at 15 kV and 10 nA with a 10 μm beam diameter. The standard materials are Mg_2SiO_4 for Si and Mg, Fe_2SiO_4 for Fe, Mn_2SiO_4 for Mn, TiO_2 for Ti and CaF_2 for F. The chemical compositions of both chondrodites are given as follows; for the natural chondrodite, 34.64 wt% SiO_2, 0.39 wt% TiO_2, 4.51 wt% FeO, 0.27 wt% MnO, 55.64 wt% MgO and 4.10 wt% F, and for the synthetic OH-chondrodite, 35.59 wt% SiO_2 and 59.09 wt% MgO. The chemical formulae of the two chondrodites are $Mg_{4.76}Fe_{0.22}Ti_{0.02}Si_{1.99}O_8(OH_{1.26}F_{0.74})$ and $Mg_{4.98}Si_{2.01}H_{2.00}O_{10}$, respectively. The hydrogen content of the natural chondrodite was calculated on the basis of OH + F = 2, and that of the OH-chondrodite was calculated from the deficits of the total weight. The sizes of single crystals used for this study were 0.06 × 0.06 × 0.04 mm^3 for the natural chondrodite and 0.05 × 0.04 × 0.03 mm^3 for the synthesized one. For high-pressure experiments, a small piece of ruby was placed with each specimen in a DAC as a pressure indicator.

X-ray measurements

A modified Merrille-Bassett type diamond anvil cell (Kudoh and Takeda, 1986) was used for the high-pressure experiments. SUS301 stainless steel circle-plates with a 200 μm hole in the center were used as a gasket. A 4:1 fluid mixture of methanol and ethanol was used as a pressure medium. Generated pressures were determined by the ruby fluorescence method (Piermarini et al., 1975).

For the natural sample, all X-ray measurements were performed using an automated four-circle X-ray diffractometer (Rigaku, AFC-7S) with graphite-monochromatised MoKα radiation (λ = 0.71069Å) operated at 50 kV and 40 mA. Cell parameters of this specimen at each pressure point (ambient, 3.8, 4.8, 5.5, 6.2 and 7.3 GPa) were determined from 18-25 centered reflections in the 2θ range between 11.3° and 30.5°. The X-ray diffraction intensities of the natural chondrodite were measured up to $\sin\theta/\lambda < 0.7$ (Å^{-1}) by the 2θ-ω scan with the fixed ϕ method at pressures of 3.8, 5.5 and 7.3 GPa. For the synthesized sample, X-ray diffraction data was measured with an automated four-circle diffractometer at the beam line BL-10A of Photon Factory, High Energy Accelerator Research Organization, Tsukuba, Japan. The wavelength of the synchrotron radiation was calibrated by the unit cell constants of a ruby standard crystal at ambient conditions (λ = 0.6985Å for 0.3 GPa, λ = 0.6970Å for 3.7 GPa, λ = 0.6998 Å for 4.2 and 5.9 GPa data sets). Cell parameters of the synthetic OH-chondrodite at each pressure point (0.3, 3.7, 4.2 and 5.9 GPa) were determined from 25 centered reflections in the 2θ range between 14.6° and 35.0°. The X-ray diffraction intensity data of the OH-chondrodite was collected up to $\sin\theta/\lambda < 0.77$-$0.82$ (Å^{-1}) by the ω-scan with the fixed ϕ method at the pressures of 3.7 and 5.9 GPa (maximum 2θ is 70° for 3.7 GPa and 65° for 5.9 GPa).

Structural refinement information

For all data sets, the reflection intensity data with $I_o > 2.0\sigma(I_o)$ was used for structural refinements. After Lorentz-polarization corrections, the intensities of symmetrically equivalent reflections were averaged in the Laue group *2/m*. Extinction corrections were applied. No absorption corrections of the crystals were applied because of the small absorption coefficient value (μ = 14.1 cm^{-1} for the natural specimen and μ = 10.2 cm^{-1} for the synthetic one) and the small size of the crystals. The initial parameters of both samples with space group $P2_1/b$ (α angle obtuse) were taken from Gibbs et al. (1970). Hydrogen positions were not refined. All calculations were performed using the teXsan crystallographic software package from Molecular Structure Corporation (1992).

In the refinement of the natural chondrodite of the ambient data set, anisotropic temperature factors were used for non-hydrogen atoms. The occupancies were refined with Mg and Fe for M1 and M2 sites, and with Fe and Ti for M3 sites. The site occupancy of O5 corresponded to (OH, F) was fixed by the EPMA result (OH : F = 63 : 37). The $\frac{1}{\sigma^2(F_o)} = \left[\sigma_c^2(F_o) + \frac{p^2}{4}(F_o)^2\right]^{-1}$ weights, where $\sigma_c^2(F_o)$ is the estimated standard deviation based on counting statistics and p is p-factor, were applied. A difference Fourier synthesis map was calculated after refinement with an overall scale factor and positional and anisotropic temperature parameters using the ambient conditions data set. A small residual peak (0.115, 0.004, 0.040), which is about 0.9Å from O5 and corresponded to the hydrogen (H1) site of Yamamoto (1977), was observed but no parameters of this site were refined.

In the refinements of high-pressure data sets, the occupancies of each M and O5 sites of the natural sample are fixed by the results of the room pressure conditions. The temperature factors of all atoms in both chondrodites are isotropic. The $\frac{1}{\sigma^2(F_o)} = \left[\sigma_c^2(F_o) + \frac{p^2}{4}(F_o)^2\right]^{-1}$

Table 1. Lattice parameters of natural chondrodite and synthesized OH-chondrodite at each pressure point

Pressure (GPa)	a (Å)	b (Å)	c (Å)	α (°)	V (Å^3)	Comments
Natural chondrodite						
0.0001	4.728 (1)	10.263 (1)	7.872 (1)	109.07 (1)	361.0 (2)	
3.8	4.700 (4)	10.140 (2)	7.782 (3)	109.01 (2)	350.6 (3)	
4.8	4.691 (4)	10.112 (2)	7.767 (2)	108.98 (2)	348.4 (3)	
5.5	4.686 (4)	10.092 (2)	7.750 (2)	108.98 (2)	346.6 (3)	
6.2	4.678 (4)	10.071 (2)	7.736 (2)	108.97 (2)	344.7 (3)	
7.3	4.666 (4)	10.047 (2)	7.722 (2)	108.97 (2)	342.3 (3)	
OH-chondrodite						
0.0001	4.752 (1)	10.350 (2)	7.914 (2)	108.71 (5)	368.7 (2)	Yamamoto (1977)
0.3	4.738 (1)	10.317 (1)	7.949 (4)	108.68 (3)	368.1 (3)	
3.7	4.711 (1)	10.239 (1)	7.821 (6)	108.65 (3)	357.5 (3)	
4.2	4.709 (1)	10.225 (1)	7.809 (4)	108.63 (2)	356.3 (2)	
5.9	4.696 (1)	10.182 (1)	7.776 (2)	108.55 (4)	352.5 (3)	

Table 2. Structural refinement information of natural chondrodite and OH-chondrodite at each pressure point

	Natural chondrodite				OH-chondrodite	
Pressure (GPa)	0.0001	3.8	5.5	7.3	3.7	5.9
Scan method	ω–2θ	ω–2θ	ω–2θ	ω–2θ	ω	ω
Collected reciprocal regions	$h\pm$, $k\pm$, $l\pm$	$h\pm$, $k\pm$, $l\pm$	$h\pm$, $k\pm$, $l\pm$	$h\pm$, $k\pm$, $l\pm$	$h\pm$, $k\pm$, $l\pm$	$h\pm$, $k\pm$, $l\pm$
Reflectons for structure refinement	822	310	305	231	273	199
Number of variable	83	35	35	35	35	35
Space Group	$P2_1/b$	$P2_1/b$	$P2_1/b$	$P2_1/b$	$P2_1/b$	$P2_1/b$
R	2.7	7.5	7.6	7.6	7.9	7.3
R_w	2.9	5.7	5.5	5.4	9.4	10.0
GOF	1.09	3.24	2.92	2.54	0.99	1.09

$R = \Sigma||F_o|-|F_c||/\Sigma|F_o|$
$Rw = [\Sigma w(|F_o|-|F_c|)^2/\Sigma w|F_o|^2]^{1/2}$
$GOF = [\Sigma w(|F_o|-|F_c|)^2/(n-m)]^{1/2}$

weights were applied for the Photon Factory's data sets of OH-chondrodite. The $\frac{1}{\sigma^2(F_o)}$ weight was used for the structural refinements of the natural chondrodite under high-pressure conditions.

Refined cell parameters of both samples are given in Table 1. The conditions of structural refinements of both samples are summarized in Table 2. Final structural parameters and the selected bond distances of both specimens are given in Tables 3a, 3b and 4, respectively.

FT-IR observation

A Fourier transform infrared (FT-IR) spectrometer (JEOL, Diamond20) with an MCT-detector was used for all infrared spectroscopic experiments of the natural chondrodite. The FT-IR spectra were measured in the spectral region from 400 to 4000 cm^{-1} with a resolution of 2 cm^{-1}. A KBr beam-splitter was used. In high-pressure FT-IR observations, a Merrille-Bassett type diamond anvil cell was used for FT-IR spectra observation under high-pressures up to 9.9 GPa. An Inconel X750 steel circle-plate was used as a gasket with a 300 μm hole in the center. Fluorinert, an inactive fluid for infrared spectra, was used as a pressure medium. Although Fluorinert changed to a vitreous state at around 4 GPa, we assumed that quasi-hydrostatic conditions were kept up to 10 GPa. Generated pressures were determined by the ruby fluorescence method (Mao et al., 1986).

Results and discussion

Axial and volume compression of natural and synthesized chondrodites

The variations of a-, b- and c- axial lengths of both samples versus pressure are plotted in Figure 1 (a, b). The axial lengths decrease linearly with increasing pressure over the investigated pressure range. The linear compressibilities of each axial length, which calculated from this data, are $\beta_a = 1.69(4) \times 10^{-3}$, $\beta_b = 2.98(4) \times 10^{-3}$

Table 3a. Final atomic coordinate of natural chondrodite and OH-chondrodite at each pressure condition

		Natural chondrodite				Synthetic OH-chondrodite	
Pressure (GPa)		0.0001	3.8	5.5	7.3	3.7	5.9
M1							
	x	0.5	0.5	0.5	0.5	0.5	0.5
	y	0.0	0.0	0.0	0.0	0.0	0.0
	z	0.5	0.5	0.5	0.5	0.5	0.5
	B_{eq}*, B_{iso}	0.57 (2)	0.69 (12)	0.86 (12)	0.70 (15)	0.55 (10)	0.48 (15)
M2							
	x	0.01020 (15)	0.0110 (18)	0.0115 (17)	0.0124 (20)	0.0044 (8)	0.0078 (12)
	y	0.17376 (7)	0.1733 (4)	0.1738 (4)	0.1745 (5)	0.1769 (5)	0.1771 (8)
	z	0.30728 (9)	0.3062 (6)	0.3059 (6)	0.3064 (7)	0.3097 (14)	0.3099 (22)
	B_{eq}*, B_{iso}	0.60 (1)	0.80 (10)	0.70 (9)	0.66 (12)	0.65 (7)	0.37 (11)
M3							
	x	0.49218 (15)	0.4900 (18)	0.4903 (18)	0.4901 (22)	0.4875 (8)	0.4881 (12)
	y	0.88661 (7)	0.8881 (5)	0.8888 (5)	0.8887 (6)	0.8856 (4)	0.8834 (8)
	z	0.07900 (10)	0.0799 (6)	0.0802 (6)	0.0811 (8)	0.0784 (14)	0.0729 (21)
	B_{eq}*, B_{iso}	0.66 (2)	0.95 (10)	0.92 (10)	0.98 (14)	0.69 (8)	0.37 (12)
Si							
	x	0.07642 (13)	0.0733 (14)	0.0743 (13)	0.0753 (16)	0.0762 (6)	0.0778 (10)
	y	0.14417 (6)	0.1456 (4)	0.1459 (4)	0.1455 (5)	0.1407 (4)	0.1400 (7)
	z	0.70390 (8)	0.7047 (6)	0.7046 (7)	0.7064 (7)	0.7014 (11)	0.6993 (18)
	B_{eq}*, B_{iso}	0.50 (1)	0.65 (8)	0.61 (8)	0.67 (10)	0.25 (6)	0.08 (10)
O1							
	x	0.7789 (3)	0.7811 (32)	0.7806 (31)	0.7838 (36)	0.7747 (16)	0.7791 (25)
	y	0.0007 (1)	-0.0028 (10)	-0.0015 (10)	-0.0025 (13)	0.0007 (10)	0.0000 (19)
	z	0.2940 (2)	0.2935 (12)	0.2940 (12)	0.2936 (16)	0.2815 (28)	0.2863 (48)
	B_{eq}*, B_{iso}	0.61 (3)	0.73 (20)	0.84 (21)	0.80 (27)	0.56 (13)	0.53 (23)
O2							
	x	0.7268 (3)	0.7166 (29)	0.7215 (29)	0.7205 (33)	0.7288 (15)	0.7284 (23)
	y	0.2409 (2)	0.2428 (11)	0.2417 (11)	0.2400 (13)	0.2419 (10)	0.2443 (17)
	z	0.1257 (2)	0.1252 (13)	0.1247 (13)	0.1211 (17)	0.1254 (32)	0.1342 (50)
	B_{eq}*, B_{iso}	0.62 (3)	1.16 (22)	1.01 (21)	0.75 (28)	0.35 (12)	0.25 (21)
O3							
	x	0.2239 (3)	0.2296 (29)	0.2281 (29)	0.2262 (34)	0.2235 (15)	0.2259 (23)
	y	0.1690 (1)	0.1725 (10)	0.1711 (9)	0.1721 (13)	0.1664 (9)	0.1660 (17)
	z	0.5289 (2)	0.5283 (13)	0.5291 (13)	0.5330 (17)	0.5253 (27)	0.5192 (45)
	B_{eq}*, B_{iso}	0.63 (3)	1.04 (23)	0.86 (22)	0.89 (29)	0.31 (12)	0.28 (22)
O4							
	x	0.2632 (3)	0.2562 (28)	0.2610 (28)	0.2621 (32)	0.2630 (15)	0.2629 (20)
	y	0.8545 (2)	0.8559 (10)	0.8545 (10)	0.8562 (15)	0.8547 (10)	0.8532 (19)
	z	0.2946 (2)	0.2970 (13)	0.2963 (13)	0.2965 (16)	0.2911 (30)	0.2830 (48)
	B_{eq}*, B_{iso}	0.60 (3)	0.87 (21)	0.85 (21)	0.98 (29)	0.71 (13)	0.18 (21)
O5							
	x	0.2599 (3)	0.2541 (30)	0.2515 (31)	0.2500 (37)	0.2642 (16)	0.2658 (26)
	y	0.0567 (1)	0.0563 (9)	0.0565 (9)	0.0550 (12)	0.0598 (10)	0.0619 (21)
	z	0.0993 (2)	0.1004 (12)	0.0986 (12)	0.0948 (17)	0.1039 (29)	0.1076 (52)
	B_{eq}*, B_{iso}	0.67 (3)	1.08 (21)	1.29 (22)	1.44 (31)	0.82 (15)	1.09 (27)

The site occpancies of each M site of the natural chondrodite are refined as $(Mg_{0.879(4)}Fe_{0.121(4)})$ for M1, $(Mg_{0.959(3)},Fe_{0.041(3)})$ for M2 and $(Mg_{0.964(6)}Ti_{0.036(6)})$ for M3.

O5 site occupancy is fixed as $(OH_{0.63}F_{0.37})$ for the natural chondrodite.

* For ambient data set of the natural sample, $B_{eq} = 8\pi^2[U_{11}(aa^*)^2 + U_{22}(bb^*)^2 + U_{33}(cc^*)^2 + 2U_{12}aa^*bb^*\cos\gamma + 2U_{13}aa^*cc^*\cos\beta + 2U_{23}bb^*cc^*\cos\alpha]/3$.

Table 3b. The anisotropic temperature factor of the natural chondrodite at ambient conditions

Pressure (GPa)	U_{11}	U_{22}	U_{33}	U_{12}	U_{13}	U_{23}
Natural chondrodite						
M1	0.0077 (5)	0.0062 (5)	0.0072 (5)	0.0007 (3)	0.0017 (3)	0.0005 (3)
M2	0.0081 (4)	0.0080 (4)	0.0070 (4)	-0.0004 (3)	0.0030 (3)	-0.0001 (2)
M3	0.0076 (4)	0.0085 (4)	0.0088 (4)	-0.0005 (3)	0.0022 (3)	0.0003 (3)
O1	0.0084 (7)	0.0070 (7)	0.0079 (7)	0.0012 (5)	0.0028 (6)	-0.0001 (6)
O2	0.0077 (7)	0.0072 (8)	0.0078 (7)	0.0000 (5)	0.0012 (6)	-0.0002 (5)
O3	0.0091 (7)	0.0068 (7)	0.0081 (7)	-0.0001 (6)	0.0029 (6)	0.0010 (6)
O4	0.0077 (7)	0.0066 (7)	0.0090 (7)	0.0001 (6)	0.0033 (6)	0.0004 (6)
O5	0.0092 (7)	0.0092 (7)	0.0076 (7)	0.0023 (5)	0.0034 (5)	0.0008 (5)

The site occpancies of each M site are refined as ($Mg_{0.879(4)}Fe_{0.121(4)}$) for M1, ($Mg_{0.959(3)}$,$Fe_{0.041(3)}$) for M2 and ($Mg_{0.964(6)}Ti_{0.036(6)}$) for M3. O5 site occupancy is fixed as ($OH_{0.63}F_{0.37}$).
General temperature factor expression: $\exp[-2\pi^2(a^{*2}U_{11}h^2 + b^{*2}U_{22}k^2 + c^{*2}U_{33}l^2 + 2a^*b^*U_{12}hk + 2a^*c^*U_{13}hl + 2b^*c^*U_{23}kl)]$.

and β_c = 2.74(5) × 10^{-3} (GPa^{-1}) for the natural chondrodite, and β_a = 2.11(18) × 10^{-3}, β_b = 2.83(18) × 10^{-3} and β_c = 3.04(38) × 10^{-3} (GPa^{-1}) for the synthetic OH-chondrodite, where the cell parameters at ambient conditions of the OH-chondrodite used in the axial compressibility calculations were quoted from Yamamoto (1977). Ross and Crichton (2001) reported the linear compressibilities of synthetic OH-chondrodite [β_a = 1.88(3) × 10^{-3}, β_b = 2.80(3) × 10^{-3} and β_c = 2.79(3) × 10^{-3} (GPa^{-1}) up to 7.8 GPa] and OH-clinohumite [β_a = 1.75(2) × 10^{-3}, β_b = 2.90(4) × 10^{-3} and β_c = 2.58(3) × 10^{-3} (GPa^{-1}), up to 8.1 GPa]. The compressions of the *b*-axis direction in the humite minerals are similar each other. The β values of the *a*- and *c*-axis of OH-chondrodite are slightly larger than those of OH-clinohumite. The compressions of the *a*- and *c*-axial directions of minerals of the humite group would be the key to understand their compression mechanism. The chondrodite structure has three octahedral sites (M1, M2 and M3) and one tetrahedral site. M2 and M3 cations are coordinated by one and two (OH, F) anions, respectively, whereas anions without bonding an (OH, F) anion, denoted as O5, bonds to M1 cation. The key structural unit of the humite minerals, which is a serrated chain of edge-sharing octahedra (for example, the 4-3-4 zigzag chain in the chondrodite structure), runs parallel to the *c*-axis (Fig. 2). These octahedral chains are connected by the TO_4 tetrahedra, which share corners. The *c*-axis corresponds to the stacking direction of the forsterite-like and brucite-like slabs. The β_c values in minerals of the humite group become more compressible as the proportion of the brucite-like slabs increase. The compression of $MgO(OH,F)_6$ octahedra would influence compression in the *c*-axis direction. The *a*-axis corresponds to the stacking direction of a slightly distorted hexagonal closest-packed array of oxygen. The tendency of the octahedra to be coordinated with hydroxyl in this polysomatic series decreases as the component of the forsterite-like slabs increase. The differences in β_a values in humite minerals might be produced by the proportion of hydroxyl in the anion packed array. Thus, comparing the β values between the natural and synthetic chondrodites, the slight differences in the compression along the *a*- and *c*- axis directions can be attributed to the replacement of F ⇔ OH caused by the differences of the ionic radii. One of the effects of the substitution of F for OH is the volume change of the octahedron coordinated with hydroxyl anions (Table 4). The decreasing ratios in the mean M2-O, M3-O distances and the M2, M3 octahedral volumes of the OH-chondrodite at 5.9 GPa are higher than those of the natural chondrodite at 7.3 GPa. Thus, the compressions of M2 and M3 octahedra in the chondrodite structure, which have hydrogen coordinated O atom, would affect the compression of the axial lengths.

Compression curves of the natural chondrodite and synthetic OH-chondrodite are plotted in Figure 3. The isothermal bulk moduli of both samples, which were calculated by the Birch-Murnaghan equation of state assuming $K_T' = 4$, were K_T = 124.1(4) GPa and K_T = 117(2) GPa, respectively. If we assume $K' = 4.9$, derived from Ross and Crichton (2001), the bulk moduli can be calculated to be obtained K_T = 121.6(5) GPa for the natural sample and K_T = 115(2) GPa for the OH-chondrodite. These values are consistent with those of Ross and Crichton (2001). Parise et al. (1998) suggested a simple correlation between the bulk modulus (K) and density (ρ) for dense hydrous magnesium silicate minerals (DHMS) and hydroxides (Fig. 4). Our results are consistent with their relationship.

Table 4. Selected bond distances (Å) and polyhedral information of natural chondrodite and synthesized OH-chondrodite

	Natural chondrodite				Synthesized OH-chondrodite		Yamamoto (1977)
Pressure (GPa)	0.0001	3.8	5.5	7.3	3.7	5.9	0.0001
SiO_4 tetrahedron							
Si-O1	1.6416 (14)	1.606 (10)	1.610 (10)	1.580 (13)	1.652 (8)	1.61 (2)	1.642
Si-O2	1.6319 (12)	1.585 (9)	1.592 (9)	1.600 (11)	1.660 (11)	1.61 (2)	1.636
Si-O3	1.637 (2)	1.656 (11)	1.631 (11)	1.610 (14)	1.64 (2)	1.66 (3)	1.637
Si-O4	1.606 (2)	1.549 (14)	1.571 (14)	1.57 (2)	1.599 (7)	1.605 (10)	1.620
Ave.	1.629 (2)	1.599 (11)	1.601 (11)	1.59 (1)	1.64 (1)	1.62 (2)	1.634
Volume (Å^3)	2.186	2.06	2.07	2.04	2.22	2.15	2.205
λ	1.010	1.01	1.01	1.01	1.01	1.01	1.010
σ^2	44.003	50.24	50.94	43.76	48.92	48.27	45.339
$M1O_6$ octahedron							
M1-O1 [x2]	2.092 (2)	2.073 (12)	2.064 (12)	2.066 (14)	2.15 (2)	2.12 (3)	2.084
M1-O3 [x2]	2.1227 (14)	2.115 (10)	2.098 (10)	2.097 (13)	2.103 (8)	2.092 (14)	2.125
M1-O4 [x2]	2.1259 (12)	2.107 (9)	2.096 (8)	2.077 (11)	2.139 (10)	2.17 (2)	2.125
Ave.	2.114 (2)	2.098 (1)	2.086 (10)	2.080 (13)	2.13 (1)	2.13 (2)	2.111
Volume (Å^3)	12.069	11.80	11.58	11.41	12.38	12.35	12.0415
λ	1.03	1.03	1.03	1.03	1.03	1.03	1.028
σ^2	103.42	103.28	107.88	121.71	96.23	92.62	100.410
$M2O_5$(OH, F) octahedron							
M2-O1	2.059 (2)	2.062 (11)	2.050 (10)	2.048 (14)	2.055 (10)	2.06 (2)	2.075
M2-O2	2.226 (2)	2.245 (12)	2.217 (12)	2.225 (14)	2.20 (2)	2.16 (2)	2.229
M2-O3	2.030 (2)	2.013 (12)	2.013 (12)	2.02 (2)	2.01 (2)	1.96 (3)	2.051
	2.1774 (14)	2.131 (11)	2.133 (11)	2.111 (14)	2.160 (8)	2.173 (14)	2.179
M2-O4	2.1728 (14)	2.172 (11)	2.134 (10)	2.130 (14)	2.169 (9)	2.16 (2)	2.196
M2-O5	2.0574 (12)	2.010 (10)	2.002 (10)	2.016 (13)	2.072 (12)	2.04 (2)	2.066
Ave.	2.120 (2)	2.106 (11)	2.092 (11)	2.09 (1)	2.11 (1)	2.09 (2)	2.133
Volume (Å^3)	12.317	12.07	11.83	11.82	12.16	11.79	12.521
λ	1.02	1.02	1.02	1.02	1.02	1.02	1.023
σ^2	76.30	73.45	73.66	76.94	70.53	72.83	76.586
$M3O_4(OH, F)_2$ octahedron							
M3-O1	2.1857 (13)	2.159 (12)	2.151 (12)	2.144 (14)	2.132 (11)	2.19 (2)	2.245
M3-O2	2.0007 (13)	1.968 (10)	1.970 (10)	1.940 (12)	1.988 (12)	2.00 (2)	2.115
	2.1202 (14)	2.129 (12)	2.117 (12)	2.109 (14)	2.105 (9)	2.11 (2)	2.138
M3-O4	2.127 (2)	2.128 (11)	2.111 (11)	2.087 (14)	2.08 (2)	2.05 (3)	2.018
M3-O5	2.024 (2)	1.997 (11)	1.995 (12)	1.99 (2)	2.025 (10)	2.03 (3)	2.056
	2.0530 (14)	2.061 (11)	2.046 (11)	2.03 (2)	2.06 (2)	2.04 (2)	2.091
Ave.	2.085 (2)	2.074 (11)	2.065 (11)	2.05 (1)	2.07 (1)	2.07 (1)	2.111
Volume (Å^3)	11.788	11.58	11.45	11.21	11.45	11.41	12.160
λ	1.02	1.02	1.02	1.02	1.02	1.02	1.022
σ^2	59.22	61.85	58.69	56.59	56.44	76.51	72.208
O5···O5[a]	2.941 (2)	2.88 (2)	2.84 (2)	2.78 (2)	3.011 (13)	3.05 (2)	3.063
O5-O5[b]	2.786 (2)	2.82 (2)	2.82 (2)	2.79 (2)	2.793 (13)	2.81 (2)	2.832

The λ and σ^2 are given after Robinson et al. (1971).
[a] Unshared O5···O5 distance related to hydrogen bonding.
[b] Shared O5-O5 edge length between M3 octahedra.
For the synthetic OH-chondrodite and Yamamoto (1977) data, (OH,F) is (OH).

Structural variations of natural chondrodite

In both the natural chondrodite with F/(OH + F) = 0.37 and the OH-chondrodite used in this study, the mean Si-O distances in the tetrahedra of both samples do not vary largely in the investigated pressure range (Table 4), indicating that the SiO_4 tetrahedra behave like a rigid body in both specimens. In contrast, the mean M-O distances of the octahedra decreased with increasing pressure (Table 4); the mean M1-O, M2-O and M3-O distances of the natural chondrodite decrease by 1.6-1.8 % for an increase in pressure up to 7.3 GPa, and those (M2 and M3) of the OH-chondrodite decreased by 1.5-2.0 % up to 5.9 GPa, but that of M1 is unchanged. The bulk moduli of each

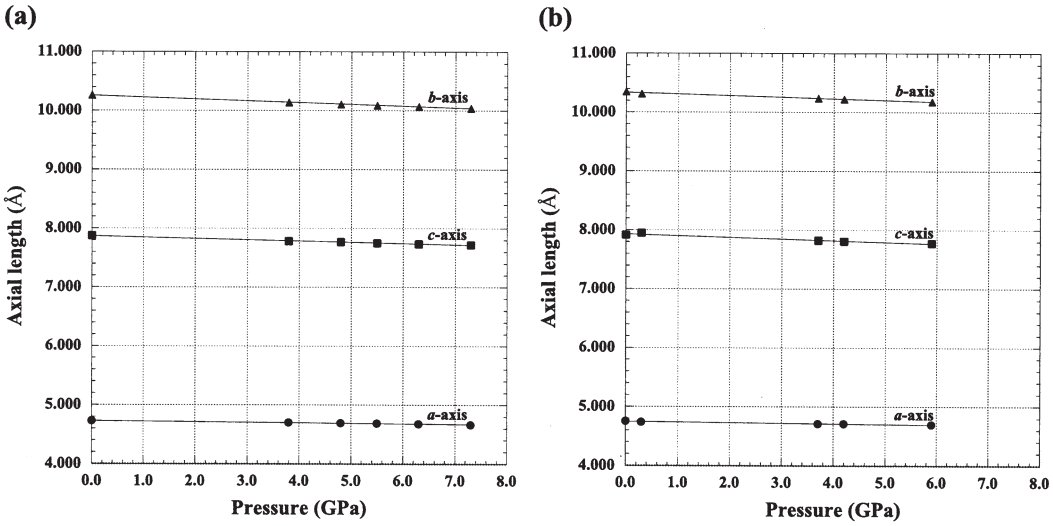

Figure 1. The variations of the *a*-, *b*- and *c*- axial lengths versus pressure in (a) natural chondrodite, and (b) OH-chondrodite.

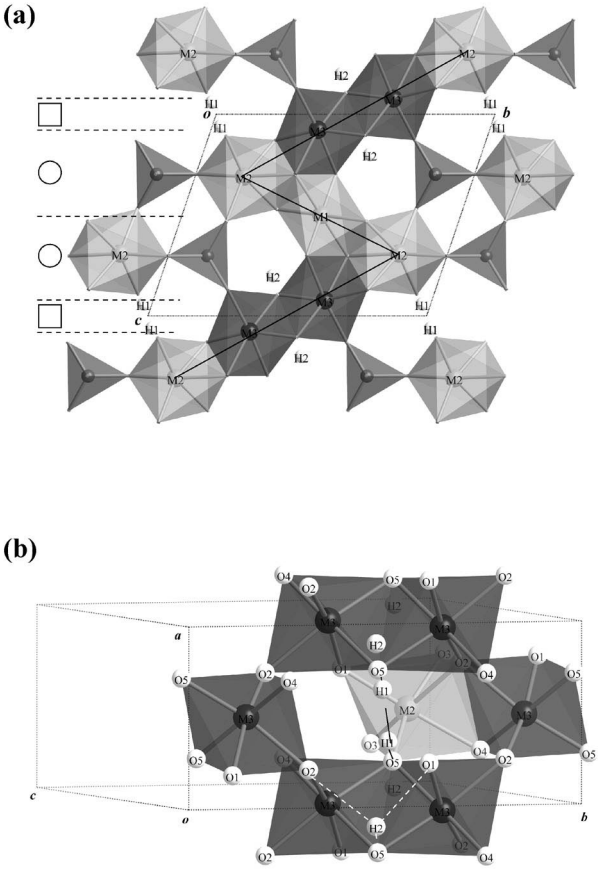

Figure 2. (a) The key structural unit of chondrodite, a serrated 4-3-4 chain of edge-sharing octahedra, running parallel to the *c*-axis (black solid line). The olivine-like slabs are marked "O", and the brucite-like slabs "□" (modified after Taylor and West, 1929). (b) Crystal structure of chondrodite surrounding the O5 site at ambient conditions. Hydrogen site data is from Yamamoto (1977). The black line shows hydrogen bonding between O5 atoms related to the H1 site. The white dashed line is related to the H2 site. The hydrogen bonding between O5 and O1 or O2 is not probably formed.

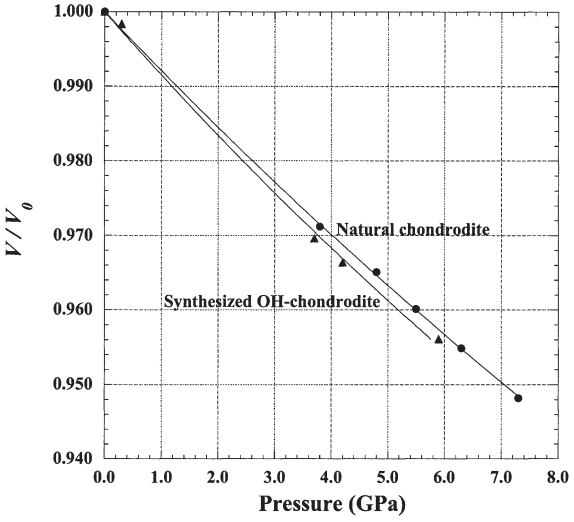

Figure 3. Compression curve of the natural chondrodite and synthetic OH-chondrodite up to 7.3 GPa. Solid circles are the data from the natural chondrodite and solid triangles are that of the synthesized OH-chondrodite.

octahedron of the present natural chondrodite with F/(OH + F) = 0.37 were calculated to be K_{M1} = 122(7), K_{M2} = 149(12) and K_{M3} = 147(15) GPa assuming $K' = 4$ using the Birch-Murnaghan equation of state. In contrast, the K_{M2} and K_{M3} values of the synthetic OH-chondrodite were 93(8) and 69(10) GPa, respectively. The K_{M1} value can not be calculated because the polyhedral volume of the M1 site was not changed in this investigated pressure range. In general, the bulk modulus of Mg octahedral site in oxide and silicate minerals is about 140-160 GPa calculated from the equation of Hazen and Finger (1982), $[\frac{K_p d^3}{S^2 z_c z_a} \approx 750\ (\text{GPa}\cdot\text{Å}^3)]$, where K_p is the polyhedral bulk

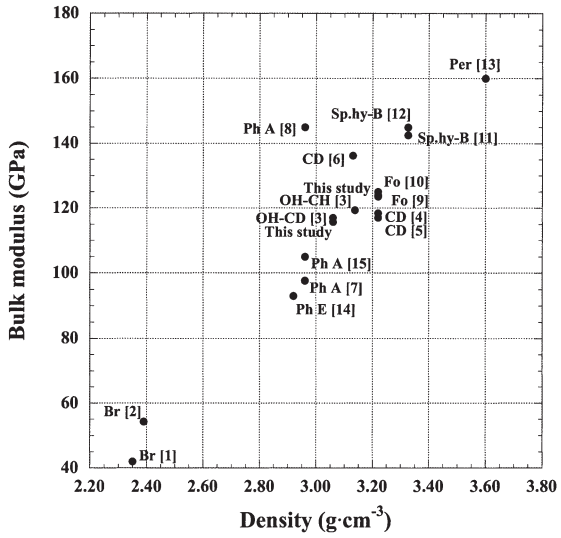

Figure 4. The relationship between the bulk modulus and density in dense hydrous magnesium silicate minerals and other hydroxides. Br, brucite; Ph E, phase E; Ph A, phase A; OH-CD, OH-chondrodite; OH-CH, OH-clinohumite; CD, natural chondrodite; Fo, forsterite; sp.hy-B, super hydrous phase B; Per, periclase. References for compression data are as follows: [1] Duffy and Ahrens (1991); [2] Fei and Mao (1993); [3] Ross and Crichton (2001); [4] Sinogeikin and Bass (1999); [5] Friedrich et al. (2002); [6] Faust and Knittle (1994); [7] Crichton and Ross (2002); [8] Pawley et al. (1995); [9] Kudoh and Takeuchi (1985); [10] Downs et al. (1996); [11] Crichton et al. (1999); [12] Kudoh et al. (1994); [13] Fei (1999); [14] Shieh et al. (2000) and [15] Kuribayashi et al. (2003)

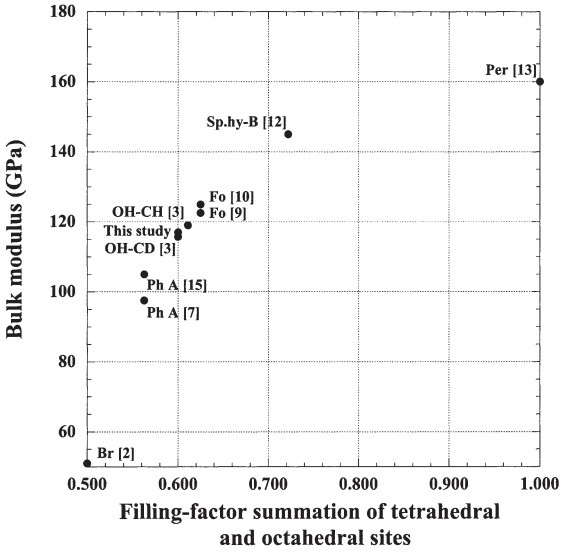

Figure 5. The variation of bulk modulus versus the summation of the filling factor of polyhedral sites in the humite minerals and some dense hydrous magnesium silicates minerals. The abbreviations and reference numbers are the same as those in Figure 4.

modulus, d is the mean cation–anion bond distance, S^2 is the "ionicity" term, in silicates, $S^2 = 0.5$, z_c is the cation formal charge and z_a is the anion formal charge. Our results show that the bulk modulus of octahedron having some hydroxyl anions becomes slightly smaller as hydroxyl anions increase.

The bulk moduli of the total void space of both samples, calculated by the Birch–Murnaghan equation of state, are $K_{\square} = 116(2)$ GPa for the natural chondrodite and $K_{\square} = 113(4)$ GPa for the OH-chondrodite, if we assume $K' = 4$. The total void space is defined as (the unit cell volume of sample) – (the summation of the volumes of each polyhedron in its unit cell). These values are slightly smaller than the bulk moduli of the respective crystals (K_T = 124 GPa and K_T = 117 GPa). In forsterite, the $K_{\square}$ value is 121(2) GPa assuming $K' = 4$ using the data of Kudoh and Takeuchi (1985). In polysomatic series such as forsterite and humite minerals, one half of "available" octahedral sites are occupied, whereas the filling rates of "available" tetrahedral sites are different (1/8 for forsterite, 1/9 for clinohumite, 3/28 for humite, 1/10 for chondrodite and 1/12 for norbergite). This is because the replacement of $Si^{4+} + 4O^{2-} \Leftrightarrow 4(OH,F)^{-} + \square$ are generated in the humite homologous series (Ribbe, 1982). The plots of bulk modulus versus the summation of the filling-factor of polyhedral sites show a good correlation for the minerals of the humite group (Fig. 5). The filling-factor (FF) is defined as fellows: FF = [the number of occupied "available" T (M) sites] / [the number of "available" T (M) sites]. In Figure 5, the FF values are in agreement perfectly between the same minerals even though the chemical compositions of the minerals are different. Hence, the difference in a vertical axis having the same FF value shows the effects of the substitution of OH ⇔ F or the other chemical composition difference. This vertical difference could correspond to the anion packing density. The packing index (P.I.) is defined as P.I. = [Σ(volume of ions)/volume of unit cell] × 10 (Berry and Mason, 1959). In this study, the P.I. was calculated on the assumption that all anions are oxygen contained in the chondrodite structure, where Shannon's ionic radii (Shannon, 1976) were used for the calculation. The difference, therefore, in the P.I. between the natural and synthetic chondrodites indicates the difference of unit cell volume between both samples, reflecting the effects of OH ⇔ F replacements on the structural variation of chondrodite. The P.I. value of the OH-chondrodite is 2% smaller than that of the natural chondrodite [F/(OH + F) = 0.37]. This difference yields the results that the bulk modulus of this natural sample [K_T = 124.1(4) GPa] is 6% larger than that of the synthetic OH-chondrodite [K_T = 117(2) GPa]. Thus, the replacements of OH ⇔ F in the chondrodite structure would affect its bulk compression.

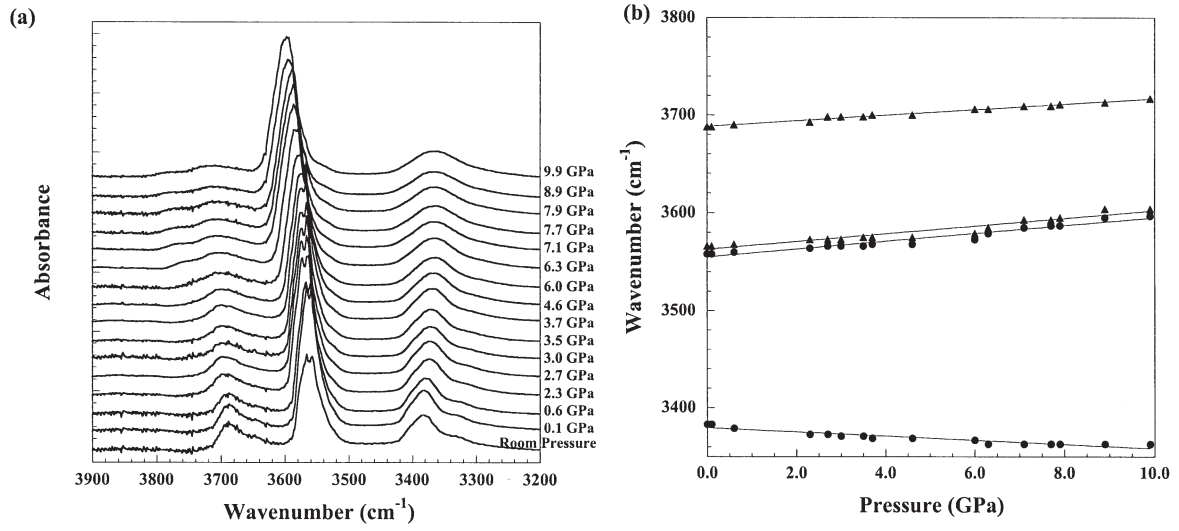

Figure 6. (a) FT-IR spectra patterns of the natural chondrodite up to 9.9 GPa at about every 1 GPa. (b) The pressure dependence of IR peaks of the natural chondrodite up to 9.9 GPa.

FT-IR observations of natural chondrodite

The variations of the FT-IR spectra of the natural chondrodite up to 9.9 GPa are shown in Figure 6 (a, b). The present FT-IR spectra pattern at ambient conditions is in good agreement with those of Williams (1992) and Cynn et al. (1996). Four OH-stretching vibration peaks are observed at 3383, 3558, 3566 and 3688 cm^{-1} at ambient conditions. The assignments of these peaks were based on the results of Cynn et al. (1996). In contrast, Akaogi and Akimoto (1986) showed that five IR spectra peaks (3465, 3530, 3570, 3615 and 3705 cm^{-1}) due to OH-stretching vibration appear in a synthesized OH-chondrodite. This difference in IR-peak position between the natural chondrodite and synthesized OH-chondrodite may show that hydrogen positions are influenced by the exchange of Mg and Fe between the M1 and M2 sites, and that of OH and F. Moreover, additional small peaks are observed at 3330 and 3653 cm^{-1}. Thus, the 3383 cm^{-1} peak in the natural chondrodite appears at a wavenumber position much lower than the corresponding peak (3465 cm^{-1}) of the synthesized OH-chondrodite ($Mg_5Si_2H_2O_{10}$; Akaogi and Akimoto, 1986). Figure 6 (a, b) show that the 3383 cm^{-1} peak shifts to a lower wavenumber (3363 cm^{-1}) with increasing pressure up to about 6 GPa, while the peaks at 3558, 3566 and 3688 cm^{-1} shift to higher wavenumber (3573, 3579 and 3706 cm^{-1}, respectively). At over 6 GPa, the weak and broad peak appears newly around 3740 cm^{-1}, but its peak position could not be determined. The $d\upsilon/dP$ values of the 3688, 3566, 3558 and 3383 cm^{-1} peaks at ambient conditions, which calculated from all data point, are 2.8(1), 3.9(3), 4.0(3) and –2.1(2) $cm^{-1}GPa^{-1}$, respectively (Fig. 6b). Williams reported that the $d\upsilon/dP$ values of the 3690, 3568 and 3382 cm^{-1} peaks of natural chondrodite [F/(OH + F) = 0.73] at ambient conditions, which corresponded to our 3688, 3566 and 3382 cm^{-1} peaks, are 1.6, 1.9 and –2.6, respectively ($cm^{-1}GPa^{-1}$). Our values are slightly larger than those of Williams (1992).

Yamamoto (1977) reported two hydrogen sites (H1 and H2) and three types of OH orientation vectors for OH-chondrodite. According to his results, both hydrogen atoms bond to O5 oxygen. H1-H1 and H2-H2 distances are 1.72 and 3.27 Å, respectively. The H1-H1 distance is so short that hydrogen atoms are statistically distributed over the two sites (H1 and H2) with 50% occupancy to avoid the H1-H1 electrostatic repulsion. The angles of O5-H1···O5 and O5-H2···O5 are about 176° and 77°, respectively. The H1 atom would form hydrogen bonds between the O5 atoms. Williams (1992) proposed that the absorption band at 3383 cm^{-1} observed in natural chondrodite would be related to the hydrogen bond involving hydroxyl attached to the M2 cation, while Cynn et al. (1996) suggested the band to the hydrogen bonding of the triangular site or the H atoms share border with oxygen other than the triangular coordinated site (*e.g.* the tetrahedral site). Thus, hydrogen bonding in the chondrodite structure was considered to exist in the separation between O5 atoms bonding to M3 and to M2.

Nakamoto et al. (1955) reported that as O-H···O hydrogen bond distance shortened, the frequency of the OH-stretching vibration changed to a lower value and vice versa. This lower shifts of OH-stretching vibration bands with increasing pressure were observed in brucite, portlandite and several other hydrous minerals under high-pressure conditions (Verde and Martinez, 1981;

Kruger et al, 1989; Shinoda and Aikawa, 1998). In the present natural chondrodite, the O5···O5 distance decreases from 2.941 to 2.78 Å (5.5 % decrease) with increasing pressure up to 7.3 GPa. This decreasing ratio is smaller than that (10% decrease) of the O···O distance related to hydrogen bonding in phase A structures up to 6.2 GPa (data from Kudoh et al., 2002; Kuribayashi et al., 2003). Although the degree of the increase in the strength of hydrogen bonding in the natural chondrodite with increasing pressure would be small compared with that of phase A, this decrease in O5···O5 distances [from 2.941(2) to 2.78(2) Å] would strengthen its related hydrogen bonding. Hence, the variation of the hydrogen position related to the unshared O5···O5 would cause the negative shift of the present IR spectrum of 3383 cm^{-1} with increasing pressure. In contrast, the shared O5–O5 edge distance (Table 4) and the other O5–O1 [3.046(2) → 3.08(2) Å], O5–O2 [2.869(2) → 2.84(2) Å] and O5–O3 [3.201(2) → 3.20(2) Å] bond distances was unchanged up to 7.3 GPa. These (O1, O2 and O3) oxygens are related to the hydrogen of the H2 site. If hydrogen bonding forms between O5 and O1 or O2 or O3, hydrogen bonding would not be strengthened significantly with an increase in pressure. At ambient condition (data from Yamamoto, 1977), the nearest H1···O4 distance is longer than 3Å and the O5–H2···O4 angle, where the H2···O4 distance is 2.66Å, is about 80°, then the hydrogen bonding should not be formed between O5 and O4. In the DHMS phase, Hofmeister et al. (1999) proposed that high frequency bands, which reflect weak hydrogen bonding, should show the positive shifts related to the compression of the O–H bonds. Lager et al. (2001) showed that the positive pressure dependence of O–H bands in F–bearing and OH– chondrodites was consistent with the existence of weak hydrogen bonds in these structures from the preliminary data of Friedrich et al. (2002) based on the model proposed by Hofmeister et al., (1999). From the results of these previous studies, it follows that the positive pressure dependence of the present IR–peaks observed at 3558, 3566 and 3688 cm^{-1} under ambient conditions is probably caused by the compression of the O5–H bond, which is related only to the M3 site.

Acknowledgments

We are grateful to Prof. Nakazawa for helpful comments and discussions. We also wish to thank Dr. Chung for the synthesized sample preparation. We appreciate two anonymous reviewers for constructive and helpful comments and discussion.

References

Akaogi, M. and Akimoto, S. (1986) Infrared spectra of high–pressure hydrous silicates in the system $MgO–SiO_2–H_2O$. Physics and Chemistry of Minerals, 13, 161–164.

Aoki, K., Fujino, K. and Akaogi, M. (1976) Titanochondrodite and titanoclinohumite derived from the upper mantle in the Buell Park kimberlite, Arizona, USA. Contributions to Mineralogy and Petrology, 56, 243–253.

Berry, L.G. and Mason, B. (1959) Mineralogy. Concepts, Description, Determinations. pp. 137, San Francisco, W. H. Freeman and Company.

Burnley, P.C. and Navrotsky, A. (1996) Synthesis of high–pressure hydrous magnesium silicates: Observations and Analysis. American Mineralogist, 81, 317–326.

Crichton, W.A., Ross, N.L. and Gasparik, T. (1999) Equation states of magnesium silicates anhydrous B and superhydrous B. Physics and Chemistry of Minerals, 26, 570–575.

Crichton, W.A. and Ross, N.L. (2002) Equation of state of dense hydrous magnesium silicate phase A, $Mg_7Si_2O_8(OH)_6$. American Mineralogist, 87, 333–338.

Cynn, H., Hofmeister, A.M., Burnley, P.C. and Navrotsky, A. (1996) Thermodynamics properties and hydrogen speciation from vibrational spectra of dense hydrous magnesium silicates. Physics and Chemistry of Minerals, 23, 361–376.

Downs, R.T., Zha, C.–S., Duffy, T.S. and Finger, L.W. (1996) The equation state of forsterite to 17.2 GPa and effects of pressure media. American Mineralogist, 81, 51–55.

Duffy, T.S. and Ahrens, T.J. (1991) The shock wave equation of state of brucite $Mg(OH)_2$. Journal of Geophysical Research, 96, 14319–14330.

Faust, J. and Knittle, E. (1994) Static compression of chondrodite: Implications for water in the upper mantle. Geophysical Research Letters, 21, 1935–1938.

Fei, Y. (1999) Effects of temperature and composition on the bulk modulus of (Mg, Fe)O. American Mineralogist, 84, 272–276.

Fei, Y. and Mao, Ho–k. (1993) Static compression of $Mg(OH)_2$ to 78 GPa at high temperature and constraints on the equation state of fluid H_2O. Journal of Geophysical Research, 98, 11875–11884.

Friedrich, A., Lager, G.A., Ulmer, P. Kunz, M. and Marshall, W.G. (2002) High–pressure single–crystal X–ray and powder neutron study of F,OH/OD–chondrodite: Compressibility, structure, and hydrogen bonding. American Mineralogist, 87, 931–939.

Fujino, K. and Takeuchi, Y. (1978) Crystal chemistry of titanian chondrodite and titanian clinohumite of high–pressure origin. American Mineralogist, 63, 535–543.

Gibbs, G.V., Ribbe, P.H. and Anderson, C.P. (1970) The crystal structures of the humite minerals II chondrodite. American Mineralogist, 55, 1182–1194.

Hazen, R.M. and Finger, L.W. (1982) Comparative Crystal Chemistry: Temperature, Pressure, Composition and the Variation of Crystal Structure. John Wiley & Sons, New York.

Hofmeister, A.M., Cynn, H., Burnley, P.C. and Meade, C. (1999) Vibrational spectra of dense, hydrous magnesium silicates at high pressure: Importance of the hydrogen bond angle. American Mineralogist, 84, 454–464.

Inoue, T., Weidner, D.J., Northrup, P.A. and Parise, J.B. (1998) Elastic properties of hydrous ringwoodite (γ–phase) in

Mg_2SiO_4. Earth and Planetary Science Letters, 160, 107-113.

Kruger, M.B., Williams, Q. and Jeanloz, R. (1989) Vibrational spectra of $Mg(OH)_2$ and $Ca(OH)_2$ under pressure. Journal of Chemical Physics, 91, 5910-5915.

Kudoh, Y. and Takeuchi, Y. (1985) The crystal structure of forsterite Mg_2SiO_4 under high pressure up to 14.9 GPa. Zeitschrift für Kristallographie, 171, 291-302.

Kudoh, Y. and Takeda, H. (1986) Single crystal X-ray diffraction study on the bond compressibility of fayalite, Fe_2SiO_4 and rutile, TiO_2 under high-pressure. Physica, 139&140B, 333-336.

Kudoh, Y., Nagase, T., Ohta, S., Sasaki, S., Kanzaki, M. and Tanaka, M. (1994) Crystal structure and compressibility of superhydrous phase B, $Mg_{20}Si_6H_8O_{36}$. In High-pressure science and Technology –1993 (Schmidt, S.C. et al. Eds.). American Institute of Physics, New York, 469-472.

Kudoh, Y., Kuribayashi, T., Kagi, H., Sasaki, S. and Tanaka, M. (2002) High-pressure structural study of phase-A, $Mg_7Si_2H_6O_{14}$ using synchrotron radiation. Journal of Physics: Condensed Matter, 14, 10491-10495.

Kuribayashi, T., Kudoh, Y. and Kagi, H. (2003) Compressibility of phase A, $Mg_7Si_2H_6O_{14}$, up to 11.2 GPa. Journal of Mineralogical and Petrological Sciences, 98, 215-234.

Lager, G.A., Ulmer, P., Miletich, R. and Marshall, W.G. (2001) O-D···O bond geometry in OD-chondrodite. American Mineralogist, 86, 176-180.

Li, B., Gawnmesia, G.D. and Liebermann, R.C. (1996) Sound velocities of olivine and beta polymorphs of Mg_2SiO_4 at Earth's transition zone pressures. Geophysical Research Letters, 23, 2259-2262.

Lin, C.-C., Liu, L.-G. and Irifune, T. (1999) High-pressure Raman spectroscopic study of chondrodite. Physics and Chemistry of Minerals, 22, 226-233.

Mao, Ho-k., Xu, J. and Bell, P.M. (1986) Calibration of the ruby pressure gauge to 800 kbar under quasi-hydrostatic conditions. Journal of Geophysical Research, 91, 4673-4676.

Nakamoto, K., Margoshes, M. and Rundle, R.E. (1955) Stretching frequencies as a function of distance in hydrogen bonds. Journal of American Chemical Society, 77, 6480-6486.

Parise, J.B., Cox, H., Kagi, H., Li, R., Marshall, W.G., Loveday, J.S. and Klotz, S. (1998) Hydrogen bonding in $M(OD)_2$ compounds under pressure. In The Review of High Pressure Science and Technology (Nakahara, M. Ed.). Proceedings of International Conference-AIRAPT-16 and HPCJ-38- on High Pressure Science and Technology, 7, 211-216.

Pawley, A.R., Redfern, S.A.T. and Wood, B.J. (1995) Thermal expansivities and compressibilities of hydrous phases in the system $MgO-SiO_2-H_2O$: talc, phase A and 10Å phase. Contributions to Mineralogy and Petrology, 122, 301-307.

Piermarini, G.V., Block, S., Bernett, J. and Forman, R.A. (1975) Calibration of the pressure dependence of the R_1 ruby fluorescence line to 195 kbar. Journal of Applied Physics, 46, 2774-2780.

Ribbe, P.H., Gibbs, G.V. and Jones, N.W. (1968) Cation and anion substitution in the humite minerals. Mineralogical Magazine, 36, 966-975.

Ribbe, P.H. (1982) The humite series and Mn-analogs, In Reviews in Mineralogy, vol.5: Orthosilicates (Ribbe, P.H. Ed.). Mineralogical Society of America, Washington, D.C., 231-274.

Robinson, K., Gibbs, G.V. and Ribbe, P.H. (1971) Quadratic elongation: A quantitative measure of distortion in coordination polyhedra. Science, 172, 567-570.

Ross, N.L. and Crichton, W.A. (2001) Compression of hydroxylclinohumite, $[Mg_9Si_4O_{16}(OH)_2]$ and hydroxylchondrodite, $[Mg_5Si_2O_8(OH)_2]$. American Mineralogist, 86, 990-996.

Shannon, R.D. (1976) Revised effective ionic radii and systematic studies of interatomic distances in halides and chalcogenides. Acta Crystallographica, A32, 751-767.

Shieh, S. R., Mao, Ho-k., Konzett, J. and Hemley, R.J. (2000) In situ high pressure X-ray diffraction of phase E to 15 GPa. American Mineralogist, 85, 765-769.

Shinoda, K. and Aikawa, N. (1998) Interlayer proton transfer in brucite under pressure by polarized spectroscopy to 5.3 GPa. Physics and Chemistry of Minerals, 25, 197-202.

Sinogeikin, S.V. and Bass, J.D. (1999) Single-crystal elastic properties of chondrodite: Implications for water in the upper mantle. Physics and Chemistry of Minerals, 26, 297-303.

Taylor, W.H. and West, J. (1929) The crystal structure of norbergite. Zeit für Kristallographie, 70, 461-474.

teXsan (1992) Crystal Structure Analysis Package. Molecular Structure Corporation, Texas, U.S.A..

Verde, B. and Martinez, G. (1981) Effects of pressure on OH-stretching frequencies in kaolinite and aluminous serpentine. American Mineralogist, 66,196-200.

Wang, J., Sinogeikin, S.V., Inoue, T. and Bass, J.D. (2003) Elastic properties of hydrous ringwoodite. American Mineralogist, 88, 1608-1611.

Williams, Q. (1992) A vibrational specrtroscopic study of hydrogen in high pressure mineral assemblages, In High-Pressure Research: Application to Earth and Planetary Sciences (Shono, Y. and Manghnani, M.H. Eds.). Geophysical Monograph Series, 67, 289-296.

Wunder, B. (1998) Equilibrium experiments in the system $MgO-SiO_2-H_2O$ (MSH): stability fields of clinohumite-OH $[Mg_9Si_4O_{16}(OH)_2]$, chondrodite-OH $[Mg_5Si_2O_8(OH)_2]$ and phase A $[Mg_7Si_2O_8(OH)_6]$. Contributions to Mineralogy and Petrology, 132, 111-120.

Yamamoto, K. (1977) The crystal structure of hydroxyl-chondrodite. Acta Crystallographica, B33, 1481-1485.

Yamamoto, K. and Akimoto, S. (1974) High pressure and high temperature investigation in the system $MgO-SiO_2-H_2O$. Journal of Solid State Chemistry, 9, 187-195.

Yamamoto, K. and Akimoto, S. (1977) The system $MgO-SiO_2-H_2O$ at high pressure and temperatures – stability fields for hydroxyl-chondrodite, hydroxyl-clinohumite and 10Å-phase. American Journal of Science, 277, 288-312.

Yusa, H. and Inoue, T. (1997) Compressibility of hydrous wadsleyite (β-phase) in Mg_2SiO_4 by high pressure X-ray diffraction. Geophysical Research Letters, 24, 1831-1834.

(Manuscript received; 30 April, 2004)
(Manuscript accepted; 30 June, 2004